

Coherent phase control in ionization of Magnesium by a bichromatic laser field of frequencies ω and 2ω

Gabriela Buică-Zloh^{1,a} and L. A. A. Nikolopoulos^{1,2}

¹ Institute of Electronic Structure and Laser, FORTH P.O. Box 1527, Heraklion-Crete 71110, Greece

² Dept. of Telecommunications Science, Univ. of Peloponnese, GR-221 00, Tripolis, Greece

the date of receipt and acceptance should be inserted later

Abstract. We have investigated the coherent phase control on the $3p^2$ autoionizing state (AIS) resonantly coupled with the ground state for Mg through a two- and a four-photon transition simultaneously, using a bichromatic linearly polarized laser field. The frequency is chosen such that the lasers are tunable around resonance with the transition $3s^2(^1S^e) \rightarrow 3p^2(^1S^e)$, which implies $\omega_f = 2.11$ eV and $\omega_h = 4.22$ eV. We are interested in the modification of autoionizing (AI) line shape through the relative phase and laser intensities. A strong phase dependence on the total ionization yield and ionization rate is found. We also performed a time-dependent calculation which takes into consideration all the resonant states of the process.

PACS. 3 2.80.Qk Coherent control of atomic interactions with photons - 32.80.Rm Multiphoton ionization and excitation to highly excited states (e.g., Rydberg states) - 32.80.Dz Autoionization

1 Introduction

This paper treats a particular aspect of the control of photoabsorption, and in particular, ionization through the relative phase of two electromagnetic fields acting simultaneously on an atomic system. The aspect in question is the possibility of altering the line shape of an autoionizing resonance through such phase control. The general features of phase control in photoabsorption have been discussed in the literature extensively [1, 2, 3, 4, 5, 6, 7]. The possibility of altering an autoionizing line shape has also been discussed [8] to some extent in theoretical work where it has been shown that one particularly intriguing feature, depending on parameters, is the possibility of turning off the transition to the "discrete" or the continuum part of the resonance [9, 10]. To the best of our knowledge, experimental observation of such an effect has not been recorded, one of the reasons perhaps being the unavailability of radiation sources of intensity and frequency suitable for convenient atomic species and resonances.

The case studied in this paper aims at presenting a quantitative analysis of a situation possibly convenient for existing laser sources whose potential in phase control has been tested experimentally. We have thus undertaken the study of the line shape of the $3p^2(^1S^e)$ autoionizing resonance of atomic Magnesium under the simultaneous excitation by four- and two-photon transitions whose relative phase is varied. This case [11] is somewhat different

from, and theoretically a bit more demanding, than the more standard scheme of one- and three-photon transitions, which in any case would not be applicable here owing to the parity of the resonance which is the same as that of the ground state. In addition, we have found that bound states in near resonance with one- or three-photon transitions introduce distortions in the wings of the autoionizing resonance; an effect not a priori obvious but which has to be taken into account for a realistic assessment of the observability of the desired feature. Needless to say that a realistic atomic structure and transitions calculation has been necessary, whose details are discussed in the sections that follow.

Lyra and Bachau [8] studied the phase control in two- and four-photon ionization of the Magnesium atom in a bichromatic field of frequencies ω and 3ω , in the vicinity of an autoionizing resonance $^1D^e$ lying above the first two ionization thresholds. Moreover, they accomplished a full perturbative, time-independent phase control calculation in Mg by interfering three- and one-photon transitions to a single continuum channel $^1P^o$. They studied the dependence of the ionization rate as a function of the relative phase for different laser intensities, and noticed that the presence of an intermediate resonance may enhance the overall ionization signal.

Kylstra *et al.* [12] have performed a non-perturbative ab-initio one- and two-color calculation of the multiphoton ionization of Magnesium, where the laser frequencies are chosen such that the initial state of the atom is resonantly coupled to the autoionizing $3p^2$, $3s3d$, and $4s5s$ resonances

^a permanent address: Institute for Space Sciences, P.O. Box MG-23, Ro 77125, Bucharest-Măgurele, Romania

of the atom. Using R-matrix Floquet theory, they studied single photon ionization from the ground state $3s^2$ and the $3s3p$ excited state of Magnesium in the vicinity of the $3p^2$ AI resonance at non-perturbative laser intensities. A second low-frequency laser couples the $3p^2$ and $3s3d$ AI states. This resonant system was studied experimentally and theoretically in the perturbative domain. Kylstra *et al.* also investigated the harmonic intensity regime where the process is no longer perturbative.

In section 2 we present the basic framework related to the study of the phase control in the vicinity of an AI state. In section 3 we briefly give the ab-initio theoretical approach for the description of the Magnesium atomic structure. Further details can be found in [13,14,15]. Finally, in section 4 we present our results.

2 Basic Equations

We study the multiphoton ionization of Mg using a realistic atomic model which describes the time-evolution of the system, investigating the phase coherent effect on the $3p^2$ ($^1S^e$) autoionizing state resonantly coupled to the ground state of Mg, simultaneously through two- and four-photon transitions, in the weak field regime. The laser frequency is such that the ground state of the atom is near resonance with the $3s3p$ ($^1P^o$) ($E_{3s3p} \approx 4.34$ eV) state of the Mg atom due to its second harmonic, and with $3s4p$ ($^1P^o$) ($E_{3s4p} \approx 6.11$ eV) due to three-photon absorption from the fundamental.

We consider the Magnesium atom consisting of a ground state $|g\rangle \equiv |3s^2\ ^1S^e\rangle$, an autoionizing state $|a\rangle \equiv |3p^2\ ^1S^e\rangle$, and one continuum corresponding to three different values of angular momentum $|c_1\rangle \equiv |3s\epsilon s\ ^1S^e\rangle$, $|c_2\rangle \equiv |3s\epsilon d\ ^1D^e\rangle$, and $|c_3\rangle \equiv |3s\epsilon g\ ^1G^e\rangle$. The AIS is modeled as a discrete state embedded into the continuum and coupled to the $^1S^e$ continuum through the configuration interaction.

In Figure 1 we show the energy diagram of the atomic system interacting with the linearly polarized bichromatic field:

$$\mathbf{E}(t) = \mathbf{E}_f(t) \exp(i\omega_f t) + \mathbf{E}_h(t) \exp(i\omega_h t + i\varphi) + cc., \quad (1)$$

consisting of a superposition between the fundamental with frequency ω_f and its second harmonic with frequency $\omega_h = 2\omega_f$. The amplitudes of the two components of the electric field are $\mathcal{E}_f(t)$, $\mathcal{E}_h(t)$, and φ is the relative phase between them. The continuum state of energy $E_g + 4\omega_f$ can be reached by the two interfering paths shown in Figure 1, namely, the four photon absorption from the fundamental electromagnetic field (Figure 1, path (i)), and the two-photon absorption of its second harmonic (Figure 1, path (ii)).

There are a few other processes which might affect the interference process, but for the intensities we consider in this paper they are not significant, therefore we do not need to include them in the calculation. For instance, a three-photon transition with two photons of the fundamental and one of the harmonic could lead to the same

final continuum energy. These processes, however, could only influence the background signal, and not the interference process, since the final continuum state belongs either to a $^1P^o$ or to a $^1F^o$ state. We have estimated the transition amplitudes for these three-photon transitions and for values of the laser intensities involved in our calculation, and we found out that the contribution to the ionization signal is about two orders of magnitude smaller than the contribution due to the processes presented in Figure 1. One can therefore conclude that these three-photon processes do not affect the process studied here and we neglect them. The dominant processes are decided by the value of the frequency and intensities involved in the calculation. For the same reason, Raman-type processes are ignored due to the fact that they represent higher-order processes with respect to the electric field. We have used atomic units throughout this work. The atomic unit used for the intensity of laser field is $I_0 = 14.037 \times 10^{16}$ W/cm².

A four photon transition from the $|3s^2\ ^1S^e\rangle$ state into the continuum leads to a final state containing $|3s\epsilon s\ ^1S^e\rangle$, $|3s\epsilon d\ ^1D^e\rangle$, and $|3s\epsilon g\ ^1G^e\rangle$ partial waves, while a two-photon transition into the continuum leads only to $|3s\epsilon s\ ^1S^e\rangle$ and $|3s\epsilon d\ ^1D^e\rangle$ partial waves. Thus, only the transition amplitude to the $^1S^e$ and $^1D^e$ continua is modulated through the interference with the two-photon amplitude. The transition amplitude to the $^1G^e$ continuum remains unaffected by the quantum interference, and therefore only contributes to the background of the total ionization signal.

We consider the Schrödinger equation:

$$i \frac{\partial \Psi(t)}{\partial t} = [H_a + D(t)] \Psi(t), \quad (2)$$

where H_a represents the atomic Hamiltonian. The atomic system is treated as a two *active* electron system: the atomic core (the nucleus and the 10 inner-shell electrons), and two valence electrons. More details about the atomic structure calculation are given in the next section. Within the semiclassical formalism, the interaction between the atom and the bichromatic field is described in the length gauge, and in the dipole approximation by $D(t) = -(\mathbf{r}_1 + \mathbf{r}_2) \cdot \mathbf{E}(t)$, where \mathbf{r}_1 and \mathbf{r}_2 represent the position vectors of the two valence electrons. In order to describe the dynamics of the system, the time dependent wavefunction is expanded in terms of the complete set of states, and then substituted into the Schrödinger equation following the standard procedure [16]. At $t = 0$ the system is assumed to be in the ground state $|g\rangle$, and for time $t > 0$ its wave function can be written as:

$$|\psi(t)\rangle = \tilde{c}_g(t)|g\rangle + \sum_{j=1}^3 \int dE_{c_j} \tilde{c}_j(t)|c_j\rangle, \quad (3)$$

where \tilde{c}_g , and \tilde{c}_j are the probability amplitudes of states $|g\rangle$ and $|c_j\rangle$, assumed to be eigenstates of the atomic Hamiltonian H_a with the eigenenergies E_g and E_{c_j} , respectively. The substitution of the wave function Eq. (3) into the Schrödinger Eq. (2) leads to a set of differential equations for the amplitude coefficients. We introduce the slowly varying coefficients $c_g = \tilde{c}_g e^{i(E_g)t}$ and

$c_j = \tilde{c}_j e^{i(E_g + 4\omega_f)t}$, and, after the adiabatic elimination of the coefficients for the continuum $|c_j\rangle$ in the differential equation for the coefficient of the ground state, using the rotating wave approximation, we are left with one independent equation (for the ground state), and three coupled differential equations governing the time evolution of the probability amplitudes as such:

$$i \frac{\partial c_g(t)}{\partial t} = \left[S_g - \frac{i}{2} \gamma_g(\varphi, t) \right] c_g(t), \quad (4)$$

$$i \frac{\partial c_j(t, E_{c_j})}{\partial t} = c_j(t, E_{c_j}) \epsilon_{c_j} \quad (5)$$

$$+ \left[D_{c_j g}^{(4)}(E_{c_j}, t) + e^{-2i\varphi} D_{c_j g}^{(2)}(E_{c_j}, t) \right] c_g(t), \quad j = 1, 2, \quad (6)$$

where $\epsilon_{c_j} = E_{c_j} - E_g - 4\omega_f$, $j = 1, 2, 3$. We used the identity:

$$\lim_{\eta \rightarrow 0^+} \int \frac{f(x)}{x - x_0 + i\eta} dx = \mathcal{P} \int \frac{f(x)}{x - x_0} dx - i\pi f(x_0), \quad (7)$$

where \mathcal{P} is the Cauchy principal value integral. S_g represents the ground state AC-Stark shift induced by the laser field. Since we are working in the weak laser field regime, S_g will be neglected.

The quantities $D_{c_j g}^{(2)}$ and $D_{c_j g}^{(4)}$ are the effective two- and four-photon transition amplitudes from the ground state $|g\rangle$ to continuum $|c_j\rangle$:

$$D_{c_j g}^{(2)}(E_{c_j}, t) = \sum_n \frac{M_{c_j n}^{(h)} M_{ng}^{(h)}}{\omega_{ng} - \omega_h}, \quad j = 1, 2 \quad (8)$$

$$D_{c_j g}^{(4)}(E_{c_j}, t) = \sum_{n, l, m} \frac{M_{c_j n}^{(f)} M_{nl}^{(f)} M_{lm}^{(f)} M_{mg}^{(f)}}{(\omega_{ng} - 3\omega_f)(\omega_{lg} - 2\omega_f)(\omega_{mg} - \omega_f)}, \quad j = 1, 2, 3, \quad (9)$$

where the one-photon transition amplitude between the state $|A\rangle$ and $|B\rangle$ are written in the length gauge as $M_{AB}^{(h)}(t) = -\langle A | (\mathbf{r}_1 + \mathbf{r}_2) \cdot \mathbf{E}_h(t) | B \rangle$, and $M_{AB}^{(f)}(t) = -\langle A | (\mathbf{r}_1 + \mathbf{r}_2) \cdot \mathbf{E}_f(t) | B \rangle$, respectively, and $\omega_{AB} = E_A - E_B$. The quantity γ_g represents the effective total ionization width directly into the continuum, from the ground state:

$$\gamma_g(\varphi, t) = 2\pi \sum_{j=1}^2 \left| \bar{D}_{gc_j}^{(4)}(t) + \bar{D}_{gc_j}^{(2)}(t) e^{2i\varphi} \right|^2 + 2\pi \left| \bar{D}_{gc_3}^{(4)}(t) \right|^2, \quad (10)$$

where the bar over the effective transition amplitudes $\bar{D}_{gc_j}^{(4)}$, and $\bar{D}_{gc_j}^{(2)}$ means that they have been calculated at $E_{c_j} = E_g + 4\omega_f$, $j = 1, 2, 3$.

Firstly, we consider the ionization probability per unit time P , which is valid for an almost square pulse $\mathcal{E}_f \equiv \mathcal{E}_f(t)$, and $\mathcal{E}_h \equiv \mathcal{E}_h(t)$. In this case, the photoionization line shape is simply obtained in terms of the transition rate without any time-dependent calculations by assuming $\partial_t c_j(t) = 0$. The ionization rate is given as the loss of

population from the ground state:

$$P = -2\text{Im}[i\partial_t c_g(t) c_g^*(t)] = \gamma_g(\varphi). \quad (11)$$

It is possible to control different ionization products through the relative phase of the laser components. The branching ratio into the j channel is defined as $B_j = P_j/P$, where the partial ionization rates P_j are:

$$P_j = 2\pi \left| \bar{D}_{gc_j}^{(4)}(t) + \bar{D}_{gc_j}^{(2)}(t) e^{2i\varphi} \right|^2, \quad j = 1, 2 \quad (12)$$

$$P_3 = 2\pi \left| \bar{D}_{gc_3}^{(4)}(t) \right|^2. \quad (13)$$

Our calculation takes into account all the important resonances with intermediate atomic states for the process studied. For the range of intensities where the two- and four-photon transition amplitudes are of comparable values, quantum interference effects of the two ionization channels would determine the modulation of the ionization signal. The photoionization signal and the AI $3p^2$ line profile can be controlled by varying the relative phase φ between the field components of the laser field $\mathbf{E}(t)$.

If we need to explicitly take into account the temporal evolution of the laser pulse, we have to integrate the time-dependent system of differential equations Eqs. (4)-(6), with the initial conditions $c_g(t=0) = 1$ and $c_j(t=0) = 0$, $j = 1, 2, 3$. The temporal pulse shape of the laser field is a sine-squared function, $\mathcal{E}_i(t) = \mathcal{E}_i \sin^2(\pi t/T)$, where $i = f, h$. The integration time for this sine squared shape pulse is taken from $t = 0$ to $t = T = \frac{2\pi}{\omega_f} n$, with n being the number of laser cycles.

Additional parameters, such as the laser pulse duration and the temporal overlap of the fundamental and harmonic pulse, may also control the ionization signal.

The total ionization probability is calculated at the end of the laser pulse: $P_{ion}(T) = 1 - |c_g(T)|^2$. We have obtained the value $\Gamma_{3p^2} \simeq 1.76 \times 10^{-3}$ a.u. for the autoionization width of the $3p^2$ AIS, and the corresponding life-time of this level is about $\tau_{3p^2} = 13.75$ fs. The total laser pulse duration used in our calculation is larger than the life-time of the AIS.

3 Atomic structure

The Hamiltonian of the Magnesium atomic system H_a is given by:

$$H_a = \sum_{i=1}^2 \left[-\frac{1}{2} \nabla_i^2 + V_l^{HF}(r_i) \right] + \frac{1}{|\mathbf{r}_1 - \mathbf{r}_2|} + V_d(\mathbf{r}_1, \mathbf{r}_2), \quad (14)$$

where $V_l^{HF}(r_i)$ is the radial Hartree-Fock potential for the closed-shell core of Magnesium (Mg^{++}), and V_d is a two-body interaction operator that includes a dielectronic effective interaction [13,17]. The characteristic feature of the Magnesium atom is the existence of a $3s^2$ valence shell, outside a closed-shell core, the excitation of which requires a much larger amount of energy compared with the first

and second ionization threshold. This allows us to explore excitation and/or ionization processes of the valence electrons, for a certain range of photon energies, without considering the closed-shell core-excitation.

At a first stage, we perform a Hartree-Fock calculation for the closed-shell core of Magnesium (Mg^{++}), thus deriving the effective Hartree-Fock potentials 'seen' by the outer electrons. At a second stage, we solve the Schrödinger equation for the valence electrons through the configuration interaction (CI) method using the Magnesium Hamiltonian defined in Eq. (14). In this case, we also add a core polarization potential acting on the valence electrons, the inclusion of which represents the influence of the core on the two valence electrons in a way very similar to that described in [13,14]. This core-polarization potential has the form $\alpha_s \{1 - \exp[-(r/r_l)^6]\} / r^4$, where α_s is the static polarizability of the doubly-ionized Mg, and the cut-off radii, r_l , for the various partial waves $l = 0, 1, 2, \dots$ [17].

Having produced the Mg^+ one-electron radial eigenstates $P_{nl}(r)$ for each partial wave $l = 0, 1, 2, \dots$, we solve the two-electron Schrödinger equation:

$$H_a \Psi^A(\mathbf{r}_1, \mathbf{r}_2) = E \Psi^A(\mathbf{r}_1, \mathbf{r}_2), \quad (15)$$

by expanding the two-electron eigenstates $\Psi^A(\mathbf{r}_1, \mathbf{r}_2)$ on the basis of LS-uncoupled two-electron antisymmetrized orbitals $\Phi_{nl'n'l'}^A(\mathbf{r}_1, \mathbf{r}_2)$, namely [14]:

$$\Psi^A(\mathbf{r}_1, \mathbf{r}_2; E_i) = \sum_{nl'n'l'} C_{nl'n'l'}(E_i) \Phi_{nl'n'l'}^A(\mathbf{r}_1, \mathbf{r}_2), \quad (16)$$

$$\Phi_{nl'n'l'}^A(\mathbf{r}_1, \mathbf{r}_2) = A_{12} \frac{P_{nl}(r_1)}{r_1} \frac{P_{n'l'}(r_2)}{r_2} Y_{LM_L}(\hat{r}_1, \hat{r}_2; l, l'), \quad (17)$$

where $\Lambda = (LM_L)$, and A_{12} is the antisymmetrization operator which ensures that the total wave function is antisymmetric with respect to interchange of the space coordinates of the two electrons. Assuming the Magnesium is initially in its ground state $|3s^2 \ ^1S^e\rangle$, and that the transitions with a linearly polarized light are well described in the dipole approximation, we only need to construct the singlet states with $S = 0$ and $M_L = 0$.

We force the wavefunction to be zero at the boundaries by selecting the basis functions $P_{nl}(r)$, and $P_{n'l'}(r)$ to be the one-electron radial solutions of Mg^+ which, by construction vanish at the boundaries. The radial functions $P_{nl}(r)$ are expanded in a B-spline basis of order n , $P_{nl}(r) = \sum_i b_i B_i(r)$, $i = 1, 2, \dots, N$, which transforms the one-electron Schrödinger equation for the Mg^+ orbitals into a system of matrix equations for the coefficients b_i [18].

Substitution of the two electron wavefunction Eq. (17) into the Schrödinger equation Eq. (15), leads to a generalized eigenvalue matrix equation, the diagonalization of which gives the coefficients $C_{nl'n'l'}(E_i)$ for each discrete eigenvalue E_i [14,15]. This choice of the basis functions $\Phi_{nl'n'l'}^A(\mathbf{r}_1, \mathbf{r}_2)$ (constructed from the radial orbitals $P_{nl}(r)$), thus leads to a discretized continuum spectrum for the Magnesium atom with a density of states basically determined from the box radius R .

Having obtained the two-electron wavefunctions $\Phi_{nl'n'l'}^A$, we calculate the effective two- and four-photon transition amplitudes Eqs. (8)-(9) within the lowest order-perturbation theory (LOPT), as well as the corresponding partial generalized N -photon cross sections leading to the $|c_j\rangle$ continuum:

$$\sigma_{gc_j}^{(N)}(\omega) = 2\pi(2\pi\alpha)^N \omega^N \left| \mathcal{M}_{gc_j}^{(N)}(\omega) \right|^2, \quad (18)$$

where ω represents the laser frequency, α the fine structure constant, and $j = 1, 2$ for $N = 2$ (two-photon cross section) and $j = 1, 2, 3$ for $N = 4$ (four-photon cross section). The effective two- and four-photon transition amplitudes are calculated, $D_{gc_j}^{(N)}(\omega) = I^{N/2} \mathcal{M}_{gc_j}^{(N)}(\omega)$, where I represents the laser field intensity. We have employed a box with the radius close to $R \approx 300$ a.u., 602 B-spline functions of order nine, and a total number of angular momenta up to $L = 4$.

4 Results and discussion

In the first part of this section we present a few results in the weak field limit for a time-independent laser pulse, in which case the ionization rate approximation is valid, and the photoionization signal is well described by the ionization rate formula Eq. (11).

Figure 2 shows the partial two-photon ionization cross sections from the ground state of the Magnesium atom leading to the $^1S^e$ (full curve) and $^1D^e$ continuum (dotted curve), as a function of the photon energy. Our results presented in Figure 2 are in agreement with the results published in the literature by Chang and Tang [19] and Kylstra *et al.* [12]. The four-photon partial cross sections from the ground state leading to the $^1S^e$ (full curve), $^1D^e$ (dotted curve), and $^1G^e$ (dashed curve) continua are presented in Figure 3. The two- and four-photon partial cross sections were calculated using Eq. (18).

The total ionization rate for the simultaneous two- and four-photon ionization from the ground state of Mg is plotted as a function of the fundamental laser frequency in Figure 4, for a relative phase $\varphi = 0^0$ (dashed line), 30^0 (dotted line), and 90^0 (full line). The laser field intensities are $I_f = 2 \times 10^{11}$ W/cm² and $I_h = 4.13 \times 10^7$ W/cm². If the two fields are in phase, there is destructive interference between the two different ionization channels illustrated in Figure 1, while there is constructive interference at $\varphi = 90^0$. This behavior of the ionization rate is due to the relative sign of the effective two- and four-photon transition amplitudes; specifically, for a fundamental laser frequency at $2.08 \text{ eV} < \omega_f < 2.15 \text{ eV}$, the effective two- and four-photon transition amplitudes from the ground state into the $^1S^e$ and $^1D^e$ continua, respectively, have opposite signs. When the laser frequency is tuned near the resonant state $3s3p$ ($\omega_h \approx 4.3$, eV) no phase effects are observed, since the ionization through two harmonic photon absorption becomes dominant over the four photon absorption, Figure 1(ii), and no interference process exists. Where the laser is tuned around the $3s4p$ state ($\omega_f \approx 2.02$ eV), channel (i) of Figure 1 is dominant.

In order to have a better view of the interference process between the two ionization channels illustrated in Figure 1, in Figure 5 we present the partial ionization rate into the $^1S^e$ (dot-dashed curve), $^1D^e$ (dotted curve) and $^1G^e$ continua (dashed curve). The full curve represents the total ionization rate when the fields are in phase, panel (a), and when the relative phase is $\varphi = 90^\circ$, panel (b). We observe that the AI $3p^2$ line profile for the two- and four-photon process is not symmetric due to the one- and three-photon transitions to the $3s3p$ and $3s4p$ near resonance states.

Figure 6(a) shows the branching ratios function of the fundamental laser frequency at $\varphi = 0^\circ$, and in panel b) for $\varphi = 90^\circ$ with the same conditions as in Figure 4. The branching ratio into the $^1S^e$ continuum is represented by the dot-dashed curve, into the $^1D^e$ continuum by the dotted curve and into the $^1G^e$ continuum by the dashed curve. As shown in panel (a), at $\varphi = 0^\circ$ for laser frequencies tuned around $3p^2$ AIS, the ionization rate into the $^1G^e$ continuum is enhanced since the laser intensities were chosen such that the two- and four-photon transition amplitudes from the ground state into the $^1S^e$ continuum cancel each other. On the other hand, at $\varphi = 90^\circ$ in panel (b) there is an enhancement of the ionization signal into the $^1S^e$ and $^1D^e$ continua. This suggests that by a judicious choice of the laser intensities, it might be possible to arrange the maximum of one ionization product to coincide with the minimum of the others, and thus to control different ionization products.

The modulation of the ionization rate as a function of the relative phase for a simultaneous two- and four-photon ionization from the ground state of Mg to the $3p^2(^1S^e)$ AIS is depicted in Figure 7, for $\omega_f = 2.11$ eV with the same laser intensities as in Figure 4. The full curve represents the total ionization rate, the dot-dashed curve is the contribution to ionization into the $^1S^e$ continuum, and the dotted curve the contribution coming from the $^1D^e$ continuum. The ionization rate into the $^1G^e$ continuum (dashed curve) is a flat line and contributes to the background of the ionization rate, which it cannot be neglected when the relative phase between the laser field components is close to $k\pi$. The ionization rate into the $^1S^e$ at $\varphi = k\pi$ is zero since the laser intensities were chosen such that the effective transition amplitudes for two- and four-photon absorption into the $^1S^e$ continuum at $\omega_f = 2.11$ eV are almost equal, and cancel each other.

We can analyze the ionization rate as a function of the harmonic intensity for fixed frequency and intensity of the fundamental. In Figure 8 we show the depth of ionization $(P_{max} - P_{min})/\frac{1}{2}(P_{max} + P_{min})$ as a function of the harmonic intensity. P_{max} represents the maximal value of the ionization rate when $\varphi = 90^\circ$, and P_{min} is the minimal value of the ionization rate when the two laser components are in phase $\varphi = 0^\circ$; the fundamental photon energy is $\omega_f = 2.11$ eV. As can be seen, an efficient coherent control in the weak field limit is obtained at $I_f = 2 \times 10^{11}$ W/cm² for the harmonic intensity in the interval $I_h \in (2 \times 10^7 \text{ W/cm}^2, 2 \times 10^8 \text{ W/cm}^2)$. Of course, good

coherent control can be obtained as well for other pairs of laser intensities.

When considering a temporal dependence of the laser pulse shape, the total ionization probability is obtained by numerically integrating the system of differential equations for the amplitude coefficients in Eqs. (4)-(6). In Figure 9 we plot the ionization yield for field intensities where the depth of modulation has a maximal value: $I_f = 2 \times 10^{11}$ W/cm² and $I_h = 5 \times 10^7$ W/cm². The ionization yield for the relative phase $\varphi = 0^\circ$ is described by the dashed curve, for $\varphi = 30^\circ$ by the dotted curve, and for $\varphi = 90^\circ$ by the full curve. The laser pulse shape is sinusoidal with a total duration of 1 ps ($n=500$).

Figures 4-7 and 9 clearly show that the AI line shape of $3p^2$ is significantly changed by the relative phase φ of the laser components. The corresponding $3p^2$ peak at $\omega_f = 2.11$ eV is diminished the most whenever the two fields are in or out of phase due to the destructive quantum interference between the two different channels, and enhanced the most whenever $\varphi = (2k+1)\pi/2$ due to the constructive interference of the two ionization pathways. The maximum and the minimum of the ionization signal differ by more than one order of magnitude.

In order to better illustrate the destructive interference between the two- and four-photon ionization processes, in Figure 10 we plot the ionization yield as a function of the fundamental laser frequency at $\varphi = 0^\circ$, and the same laser intensities as in Figure 9. The laser pulse shape is sinusoidal with a total duration of about 1 ps. The dashed line represents the ionization rate corresponding to the four-photon absorption from the fundamental, and the dotted line describes the ionization yield due to the two-photon absorption of its second harmonic. The full line is the total ionization yield resulting from the destructive interference of these two processes.

5 Conclusion

In this paper, we have investigated the phase coherent effect of the $3p^2(^1S^e)$ autoionizing state resonantly coupled to the ground state of a Mg atom in the presence of a bichromatic laser field of frequencies ω_f and $2\omega_f$. The transition amplitudes have been evaluated using a realistic atomic structure calculation. The motivation for this study was the investigation of the possibility of achieving coherent control of the photoelectron current and changes in the autoionization line shape. We have calculated and presented, for the first time (to the best of our knowledge), four-photon partial transition amplitudes for the Mg atomic system, and the corresponding partial ionization cross sections. We have found out that the near resonance, double excited states $3s3p(^1P^o)$ and $3s4p(^1P^o)$ of Magnesium introduce distortions in the left and in the right side of the autoionizing resonance, and enhance the overall ionization signal. A reliable study of the $3p^2$ line shape through the density matrix or resolvent operator method should take into consideration these two intermediate resonances, and the energy dependence of the respective transition amplitudes and Rabi frequencies. The rel-

ative phase φ between the two components of the bichromatic laser field modulates the quantum interference between the two ionization channels: four-photon absorption from the fundamental laser field and two-photon absorption of its second harmonic.

The work by G.B-Z. was supported by the European Research Network Program Contract No HPRN-CT-1999-00129. One of the authors (G.B-Z.) is indebted to Professor P. Lambropoulos for useful discussions.

References

1. M. Shapiro, J. W. Hepburn, and P. Brumer, Chem. Phys. Lett. **149**, 451 (1988)
2. C. Chen, Y. Yin, and D. S. Elliott, Phys. Rev. Lett. **64**, 507 (1990)
3. C. Chen and D. S. Elliott, Phys. Rev. A **53**, 272 (1996)
4. N. E. Karapanagioti, D. Xenakis, D. Charalambidis, and C. Fotakis, J. Phys. B **29**, 3599 (1996)
5. S. Cavalieri, R. Eramo, and L. Fini Phys. Rev. A **55**, 2941 (1997)
6. T. Nakajima, J. Zhang, and P. Lambropoulos, J. Phys. B **30**, 1077 (1997)
7. D. B. Milosevic and F. Ehlotzky, Phys. Rev. A **57**, 2859 (1998)
8. A. Lyras and H. Bachau, Phys. Rev. A **60**, 4781 (1999)
9. T. Nakajima and P. Lambropoulos, Phys. Rev. A **50**, 595 (1994)
10. T. Nakajima and P. Lambropoulos, Phys. Rev. Lett. **70**, 1081 (1993)
11. E. Papastathopoulos, D. Xenakis, and D. Charalambidis, Phys. Rev. A **59**, 4840 (1999)
12. N.J. Kylstra, H.W. van der Hart, P.G. Burke and C.J. Joachain, J. Phys. B **31**, 3089 (1998)
13. T.N. Chang, *Many-body theory of Atomic Structure and Photoionization*, (World Scientific, Singapore, 1993), p. 213.
14. L. A. A. Nikolopoulos, Comp. Phys. Comm. **150**, 140 (2003)
15. P. Lambropoulos, P. Maragakis, and Jian Zhang, Physics Report **305**, 203 (1998)
16. P. Lambropoulos and P. Zoller, Phys. Rev. A **24**, 379 (1981)
17. S. Mengali and R. Moccia, J. Phys. B **29**, 1597, (1996)
18. H. Bachau, E. Cormier, P. Decleva, J.E. Hansen, and F. Martin, Rep. Prog. Phys. **64**, 1601 (2001)
19. T.N. Chang and X. Tang, Phys. Rev. A **46**, R2209 (1992)

TABLE - FIGURE CAPTIONS

Fig. 1. Energy diagram of the Mg atom interacting with a bichromatic electromagnetic field, showing the relevant levels for the studied process.

Fig. 2. Two-photon ionization cross section $\sigma^{(2)}$, leading to $^1S^e$ (full line) and $^1D^e$ (dotted line) continua from the ground state of Mg, as a function of the photoelectron energy.

Fig. 3. Four-photon generalized ionization cross section $\sigma^{(4)}$, leading to $^1S^e$ (full line), $^1D^e$ (dotted line) and $^1G^e$ (dashed line) continua from the ground state of Mg, as a function of the photoelectron energy.

Fig. 4. The ionization rate of the ground state of Mg as a function of the fundamental laser frequency for $\varphi = 0^0$ (dashed line), 30^0 (dotted line), and 90^0 (full line). The peak occurring at 2.02 eV corresponds to the $3s4p$ level, and the peak at 2.15 eV corresponds to the $3s3p$ level. The fundamental and harmonic laser intensity are $I_f = 2 \times 10^{11}$ W/cm² and $I_h = 4.13 \times 10^7$ W/cm², respectively.

Fig. 5. The total and the partial ionization rates of the ground state of Mg as a function of the fundamental laser frequency. In panel (a) the relative phase between field components is 0^0 , and is 90^0 in panel (b). The partial ionization rate into the $^1S^e$ continuum is represented by the dot-dashed curve, into the $^1D^e$ continuum by the dotted curve and into the $^1G^e$ continuum by the dashed curve. The full line represents the total ionization rate. The laser parameters are the same as in Figure 4.

Fig. 6. Branching ratios as a function of the fundamental laser frequency at $\varphi = 0^0$ in panel (a), and at $\varphi = 90^0$ in panel (b). The branching ratio into the $^1S^e$ continuum is represented by the dot-dashed curve, into the $^1D^e$ continuum by the dotted curve, and into the $^1G^e$ continuum by the dashed curve. The laser parameters are the same as in Figure 4.

Fig. 7. Ionization rate vs the relative phase between laser components. The laser intensities are the same as in Figure 4. The partial ionization rate into the $^1S^e$ continuum is represented by the dot-dashed curve, into the $^1D^e$ continuum by the dotted curve and into the $^1G^e$ continuum by the dashed curve. The full line represents the total ionization rate.

Fig. 8. The depth of modulation as a function of the harmonic intensity. The fundamental laser intensity is $I_f = 2 \times 10^{11}$ W/cm².

Fig. 9. The ionization yield of the ground state of Mg around the $3p^2$ AIS function of the fundamental laser frequency for $\varphi = 0^0$ (dashed line), 30^0 (dotted line), and 90^0 (full line). The fundamental and harmonic peak laser intensity are $I_f = 2 \times 10^{11}$ W/cm² and $I_h = 5 \times 10^7$ W/cm², respectively. The laser pulse shape is sinusoidal with a total duration of 1 ps.

Fig. 10. The ionization yield at $\varphi = 0^0$ as a function of the fundamental laser frequency (full curve). The dotted curve represents the ionization yield for the two-photon absorption, and the dashed one corresponds to the four-photon absorption. The peak laser intensities are the same as in Figure 9.

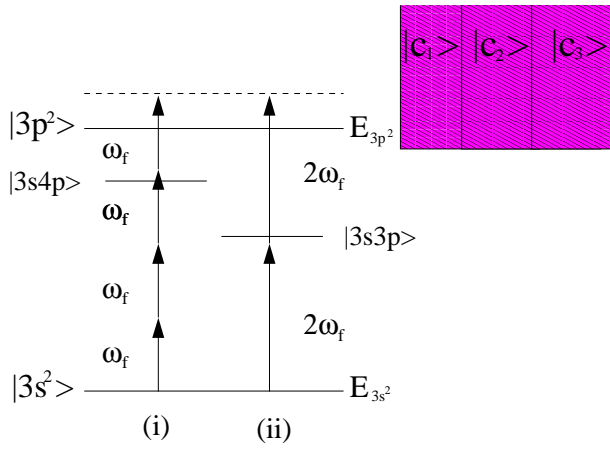


Fig. 1.

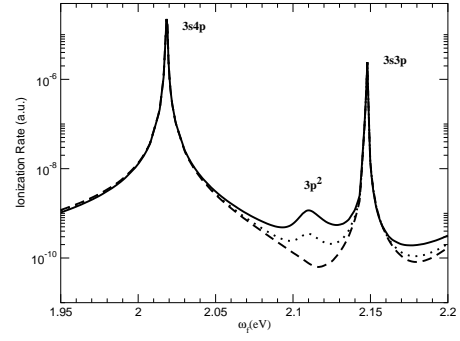


Fig. 4.

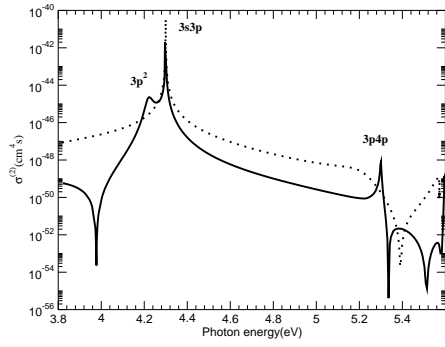


Fig. 2.

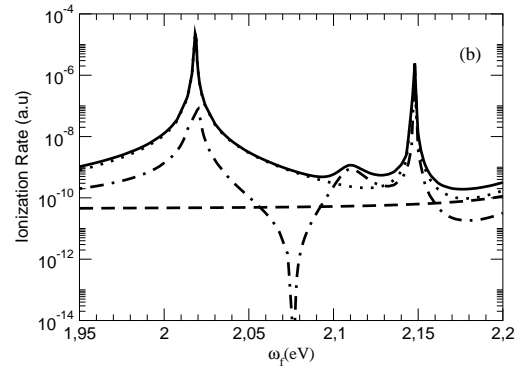
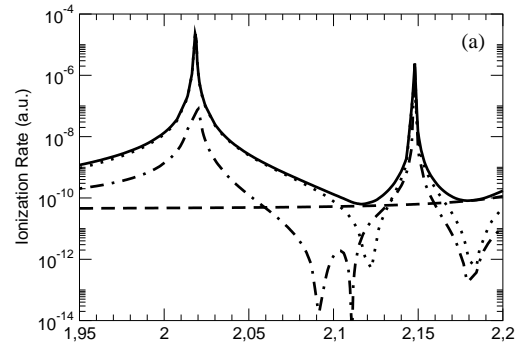


Fig. 5.

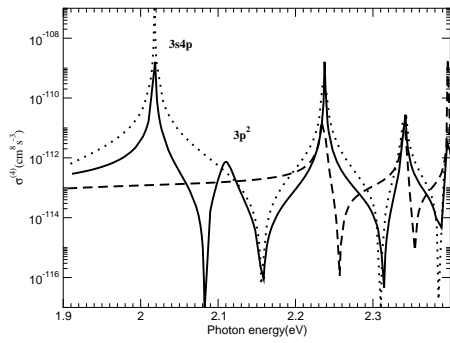


Fig. 3.

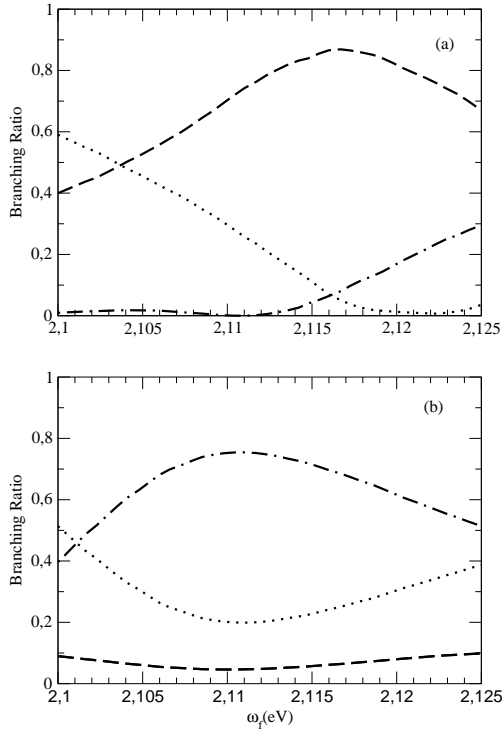


Fig. 6.

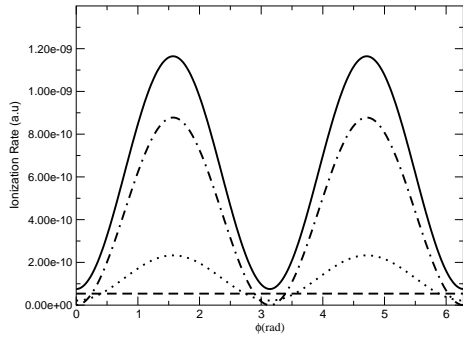


Fig. 7.

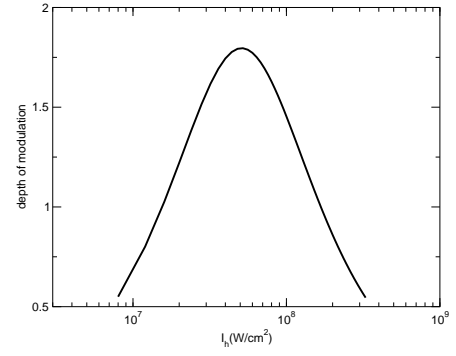


Fig. 8.

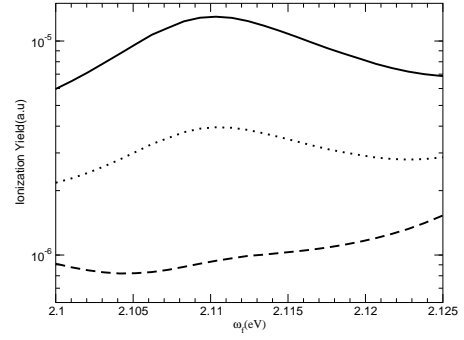


Fig. 9.

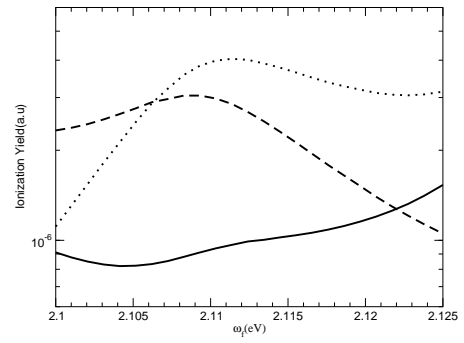


Fig. 10.